

# Controlling externally solidified crystals and porosity for enhancing mechanical properties of a die-casting aluminum-silicon alloy

Yi-hui Zhang<sup>1</sup>, \*Xiang-yi Jiao<sup>1,2</sup>, Peng-yue Wang<sup>3</sup>, Yi-xian Liu<sup>4</sup>, Jin-rui Wang<sup>4</sup>, Wen-ning Liu<sup>5</sup>, Li-jun Shi<sup>3</sup>, Cheng-gang Wang<sup>3</sup>, and \*\*Shou-mei Xiong<sup>4</sup>

1. School of Materials Science and Engineering, Northeastern University, Shenyang 110819, China

2. Key Laboratory of Lightweight Structural Materials, Liaoning Province, Northeastern University, Shenyang 110819, China

3. China FAW Foundry Co., Ltd., Changchun 130013, China

4. School of Materials Science and Engineering, Tsinghua University, Beijing 100084, China

5. Automotive Product Strategy and New Technology Research Institute, BYD Auto Industry Company Limited, Shenzhen 518118, Guangdong, China

Copyright © 2025 Foundry Journal Agency

**Abstract:** The effects of the high pressure die casting (HPDC) processes on porosity, microstructure, and mechanical properties of heat-treatment-free aluminum silicon (Al-Si) alloys have long been a focal point in automotive die-casting research. In this work, the combined effect of shot sleeve materials and slow shot speeds on porosity, microstructure and mechanical properties of a newly designed HPDC Al-Si alloy was investigated. Results show that employing a ceramic shot sleeve or increasing the slow shot speed significantly reduces both the average size and area fraction of externally solidified crystals (ESCs), as well as the average pore size and volume fraction. When the slow shot speed is increased from 0.05 m·s<sup>-1</sup> to 0.1 m·s<sup>-1</sup>, the pore volume fraction decreases by 10.2% in steel-shot-sleeve samples, compared to a substantial 67.1% reduction in ceramic-shot-sleeve samples. At a slow shot speed of 0.1 m·s<sup>-1</sup>, castings produced with a ceramic shot sleeve exhibit superior mechanical properties: 8.3% higher yield strength, 17.4% greater tensile strength, and an 81.4% improvement in elongation, relative to those from a steel shot sleeve. These findings provide valuable insights for minimizing porosity and coarse ESCs in die castings, offering promising potential for broader industrial applications.

**Keywords:** high pressure die casting; aluminum-silicon alloy; externally solidified crystals; porosity; shot sleeve

CLC numbers: TG146.21

Document code: A

Article ID: 1672-6421(2026)01-094-07

## 1 Introduction

As energy consumption and environmental issues grow more pressing, energy-saving and environmental protection have emerged as top priorities for automobile manufacturers<sup>[1-3]</sup>. Automobile lightweighting is a long-established effective approach to cut emissions in the automotive sector. Statistics show that a 10% reduction

in vehicle body weight can slash fuel consumption by about 7%, bringing significant environmental benefits<sup>[4,5]</sup>. Aluminum alloys, featuring low density, excellent corrosion resistance, and high specific strength, meet the requirements for automotive lightweighting<sup>[6]</sup>. Aluminum alloys have emerged as crucial alternatives to traditional steels in the automotive industry<sup>[7,8]</sup>.

High pressure die casting (HPDC) is an environmentally friendly metal casting process characterized by the rapid injection of molten metal from the shot sleeve into the mold under high pressure<sup>[9]</sup>. It combines high production efficiency with high accuracy casting dimensions and excellent surface quality<sup>[10,11]</sup>. However, due to its high-speed filling characteristics, there are many defects in the HPDC workpieces. A major shortcoming of HPDC is the formation of numerous pores<sup>[12]</sup>. Li et al.<sup>[13]</sup> used X-ray tomography

### \*Xiang-yi Jiao

Ph. D. His research interests primarily focus on die-casting aluminum alloy materials. To date, he has published over 20 papers in SCI indexed journals and hosted a project funded by the National Natural Science Foundation of China.

E-mail: jiaoxiangyi@mail.neu.edu.cn

### \*\*Shou-mei Xiong

E-mail: smxiong@tsinghua.edu.cn

Received: 2024-07-12; Revised: 2025-02-07; Accepted: 2025-04-08

to characterize the porosity of AM60B alloy and they found gas-shrinkage pore and net-shrinkage are the main crack sources which promote the crack propagation along the boundary of externally solidified crystals (ESCs). Liu et al.<sup>[14]</sup> studied the effects of porosity distribution and maximum pore volume on the tensile properties of HPDC Al-Si-Mn-Mg alloy, and it concluded that the pore with the largest volume in the sample was the main factor affecting the ductility. Yang et al.<sup>[15]</sup> studied the effect of porosity on the mechanical properties of HPDC Al-7Si-0.2Mg thin-plates and the results showed that porosity had a significant effect on the elongation of the alloy. In addition, ESCs are also non-negligible defects in HPDC aluminum alloys. ESCs are formed in the shot sleeve, which is a kind of coarse primary phase. In our previous work<sup>[16]</sup>, it is found the coarse ESCs promoted the formation of pores and reduced the mechanical properties of the material. Zheng et al.<sup>[17]</sup> studied the synergistic effect of ESCs and iron-rich phases on the fracture behavior of HPDC Al-8Si-0.4Mg-2Zn alloy using in-situ tensile test. The results revealed that the localized stress concentration during tensile test was significantly depended on the characteristics of ESCs and iron-rich phases. The crack preferentially initiated in the area where the fine iron-rich phase was surrounded by the clustered ESCs. Zhang et al.<sup>[18]</sup> studied the effect of porosity characteristics on the mechanical properties of HPDC AlSi7MgMn alloy. The morphology and 3D distribution of pores in tensile samples were characterized by micro-computed tomography. The results showed that the change of mechanical properties was related to the size and total volume of pores. When the maximum size of pores was reduced to less than 0.3 mm, the elongation of the alloy was increased by 13.5% at most. In the shot sleeve, the liquid metal undergoes two processes with different speed stages<sup>[19]</sup>. Under the impetus of the punch, the molten metal moves forward at a lower speed. In this process, the important parameter is the slow shot speed. The lower slow shot speed prolongs the remaining time of melt in the shot sleeve.

In addition, the materials of shot sleeves have a substantial impact on casting performances. HPDC commonly employs a steel shot sleeve which usually leads to many drawbacks. Mitrović et al.<sup>[20]</sup> designed a new Si-Mo cast iron formulation for HPDC shot sleeves. By directly reducing Fe dissolution, this innovation leads to remarkable improvements in the mechanical properties of Al castings. However, the high thermal conductivity between the molten metal and the steel shot sleeve in HPDC process leads to a rapid drop in the temperature of the molten metal. This relatively fast heat transfer between the melt and the shot sleeve material is a primary factor contributing

to the early nucleation of primary  $\alpha$ -Al within the shot sleeve. As a result, a large number of coarse ESCs are formed, which significantly undermines the performance of the castings.

In our previous work<sup>[21]</sup>, a newly designed ceramic shot sleeve was proposed for applying in HPDC AlMg6Si2MnZr alloy to control the coarse ESCs. Excellent results have been achieved in both microstructure and mechanical properties of samples produced by ceramic shot sleeve compared to the counterpart produced by steel shot sleeve. To expedite the industrial adoption of integrated die-casting alloys, it is crucial to investigate the impact of shot sleeve materials on the microstructure and mechanical properties of heat-treated free-hypoeutectic aluminum-silicon alloys.

At present, the investigation on synergetic optimized shot sleeve materials and slow shot speeds is rather limited. In this study, THAS-3 (AlSi9MnVTiMgZn) alloy was used in the experiment. Steel and ceramic shot sleeve materials were used to carry out HPDC experiments under different slow shot speed conditions. The combined effect of shot sleeve materials and slow shot speeds on microstructure, porosity, and mechanical properties of the HPDC alloy was investigated. Furthermore, the processing parameters beneficial to improving the mechanical properties of the castings were explored.

## 2 Experimental

### 2.1 Materials and process parameters

In this experiment, THAS-3 (AlSi9MnVTiMgZn) alloy was used as experimental HPDC aluminum alloy materials and its chemical compositions are shown in Table 1.

TOYO-BD-350V5 die casting machine equipped with a designed vacuum system was used to carry out die casting experiments. Figure 1(a) shows the schematic diagram of the die castings (including three bars and one plate). Figure 1(b) shows the detailed dimensions of the plate samples, which were used to study the microstructure and mechanical properties. In this experiment, the newly designed ceramic shot sleeve [Fig. 1(c)] has a three-layer structure. The outer layer of SKD61 mold steel provides durability and resists high-temperature fatigue. The middle LX metal layer, combined with the innermost nitrided layer, enhances the shot sleeve's hardness, wear resistance, and insulation (refer to Ref. [21]). The thermal conductivity of the inner shot sleeve material is lower, which can better maintain the superheat of the liquid alloy and reduce the ESCs. Table 2 lists the process parameters of die casting in this experiment, focusing on the varied slow shot speeds and shot sleeve materials: ceramic and steel.

**Table 1: Chemical compositions of AlSi9MnVTiMgZn alloy (wt.%)**

Element	Si	Mn	Fe	Cu	V	Ti	Zn	Mg	Others	Al
Nominal	8.50–9.50	0.25–0.35	0.10–0.20	≤0.2	0.15–0.25	0.05–0.15	0.15–0.25	0.15–0.25	<0.5	Bal.
Measured	9.218	0.298	0.122	0.009	0.19	0.076	0.209	0.176	0.17	Bal.

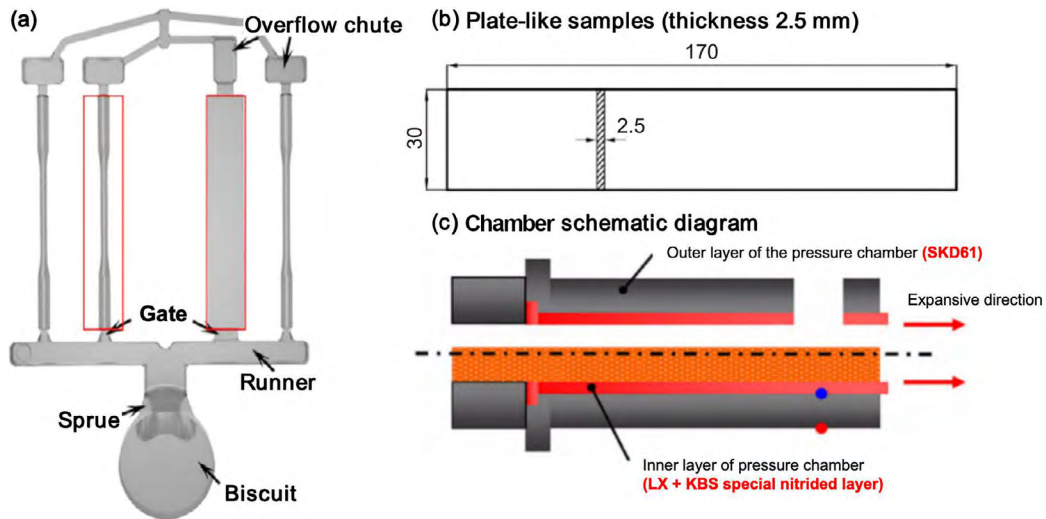


Fig. 1: Schematic diagram: (a) die casting<sup>[9]</sup>; (b) standard mechanical properties tensile plate; and (c) shot sleeve<sup>[21]</sup>

Table 2: Key HPDC processing parameters in this experiment

Material of shot sleeve	Experiment No.	Slow shot speed (m·s <sup>-1</sup> )	Fast shot speed (m·s <sup>-1</sup> )
Ceramic shot sleeve	T3	0.1	2.75
	T4	0.05	2.75
Steel shot sleeve	T23	0.1	2.75
	T24	0.05	2.75

## 2.2 Microstructure observation

The samples were grounded by #400–#2000 sandpapers, and then polished with 2.5 μm diamond polishing paste. After corrosion by 0.5vol.% HF, the samples were observed using optical microscopy (OM) and scanning electron microscopy (SEM). ESCs exhibit great difference in grain size and morphology. Therefore, to precisely quantify the size and area fraction of ESCs, Avizo software was employed, as illustrated in Figs. 2(a) and (b).

To observe and count porosity in castings, a GE lab nano CT scanner was employed. The scanning voltage and current

used in the experiment were 110 kV and 100 μA, respectively. Avizo software was used to process the reconstructed images and analyze the data. The tensile test was carried out with 1 mm·min<sup>-1</sup> tensile rate. The fracture morphology of the tensile plate was observed using SEM and lab nano CT.

## 3 Results and discussion

### 3.1 As-cast microstructure

Figure 3 show the optical micrographs of THAS-3 alloy with varied slow shot speeds and shot sleeve materials. It is clearly evident that both the slow shot speed and the shot sleeve material have a significant impact on the morphology and area fraction of ESCs. When the shot sleeve material remains constant, a decrease in the slow shot speed results in the coarsening of ESCs [Figs. 3(a) and (b)]. Simultaneously, the shape of ESCs transforms from smaller equiaxed grains to dendrites. Additionally, the shot sleeve material is another factor that influences the ESCs. As observed, the size of the ESCs in T23 is notably larger than that in T3 [Figs. 3(a) and (c)], and this size further increases with a decrease in the slow shot speed [Fig. 3(d)].

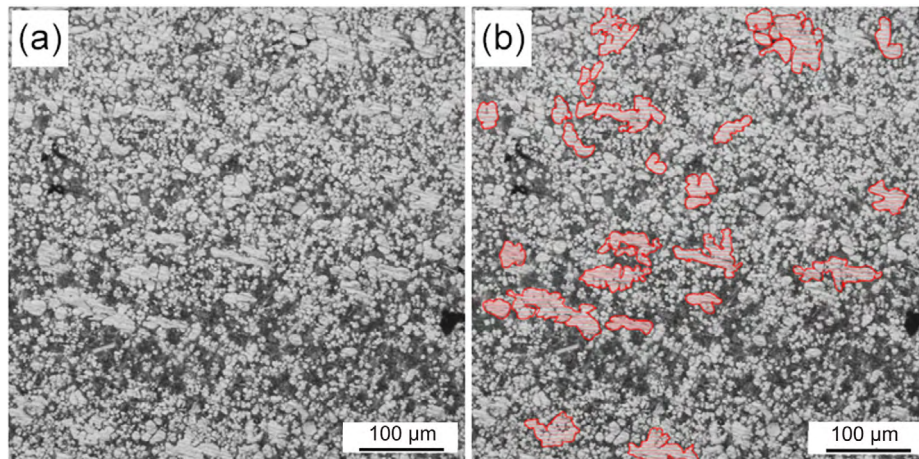
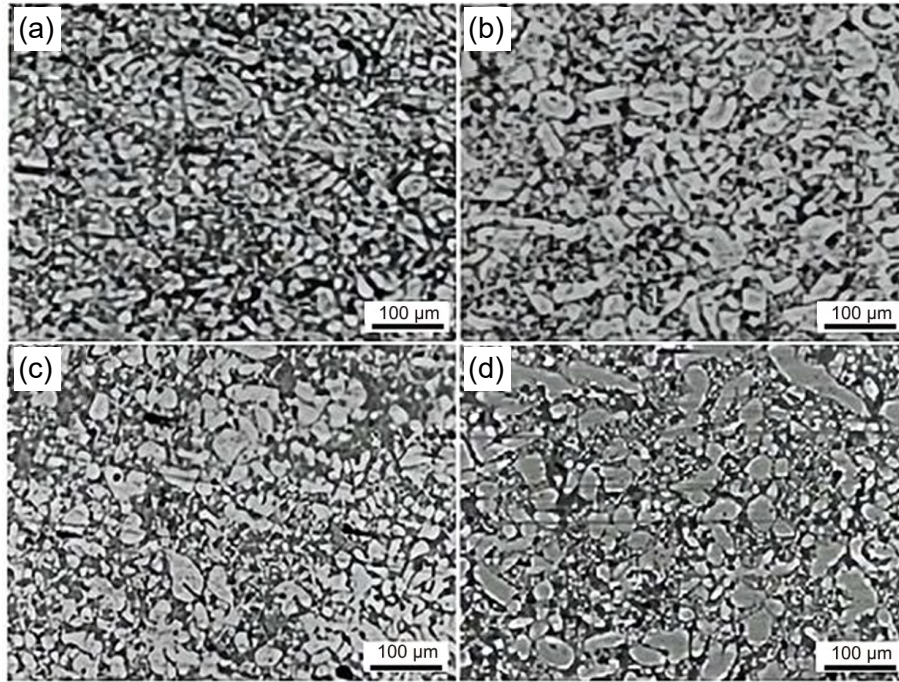


Fig. 2: Optical micrograph (a) and corresponding marked ESCs (b)



**Fig. 3: Optical micrographs of THAS-3 alloy with varied slow shot speeds and shot sleeve materials: (a) 0.1 m·s<sup>-1</sup>, ceramic shot sleeve (T3); (b) 0.05 m·s<sup>-1</sup>, ceramic shot sleeve (T4); (c) 0.1 m·s<sup>-1</sup>, steel shot sleeve (T23); (d) 0.05 m·s<sup>-1</sup>, steel shot sleeve (T24)**

In Section 2.1, it is noted that the ceramic shot sleeve employed in this experiment features an internal structure comprising LX metal and a specialized nitride layer. Significantly, its thermal conductivity is substantially lower than that of steel shot sleeve. As a result, for the high-temperature liquid metal contained within the ceramic shot sleeve, heat transfer to the exterior occurs at a slower rate. This leads to a more gradual decline in the temperature of the liquid metal. For ESCs structure, the nucleation driven force ( $\Delta G$ ) can be expressed as<sup>[21-23]</sup>:

$$\Delta G = -\frac{L_m \Delta T}{T_m} \quad (1)$$

where  $L_m$  is the latent heat,  $\Delta T$  is supercooling, and  $T_m$  is the melt point. The ceramic shot sleeve exhibits outstanding thermal insulation properties. This effectively restricts the  $\Delta T$ . As a consequence, the nucleation driving force imparted to the molten metal inside the ceramic shot sleeve is reduced. A lower nucleation driving force leads to a decrease in the quantity of primary  $\alpha$ -Al. As a result, the internal structure contains a relatively small number of ESCs, each with a comparatively small size.

Figure 4 shows the average size and area fraction of ESCs inside the samples under different process conditions and shot sleeve materials. On the whole, the average size and area fraction of ESCs in the samples using the ceramic shot sleeve are much smaller than those using the steel shot sleeve. When comparing T3 samples with T23 samples, it is evident that at a low shot speed of 0.1 m·s<sup>-1</sup>, the area fraction of ESCs in the ceramic shot sleeve drops by 52.3%. Concurrently, the average size of ESCs shrinks by 6.9%. In addition, the slow shot speed also has a significant effect on the ESCs. As the slow

shot speed increases, both the average size and the quantity of ESCs within the material generally decline.

Figure 5 shows the ESCs calibration diagram of the HPDC samples from the surface to the center. Distinct colors denote different grain sizes of ESCs. Specifically, red corresponds to grains of extremely large dimensions. A large number of ESCs in Fig. 5(a) exhibit small-sized round crystal grain. With the decrease of slow shot speed, the area fraction of ESCs increases and most of their morphologies develop into dendrites [Fig. 5(b)]. Compared with the ceramic shot sleeve, the samples prepared by the steel shot sleeve exhibit a higher area fraction of ESCs with larger-sized and more developed dendritic morphology [Figs. 5(c) and (d)]. In Fig. 5(d), ESCs tend to be enriched in the central region under the impact of liquid flow and coarse ESCs dendrites are entangled with each other to form a dendrite network.

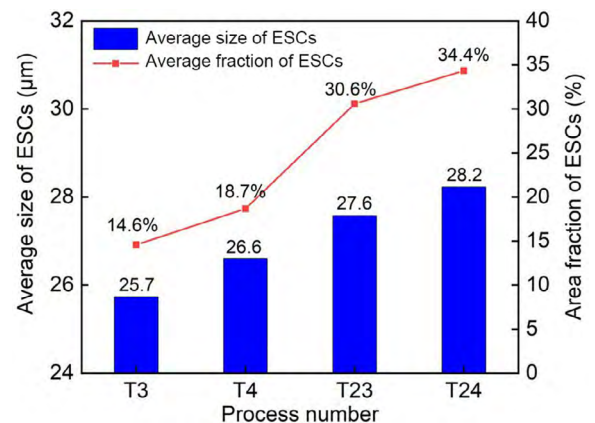


**Fig. 4: Statistics of average area fraction and average size of ESCs**

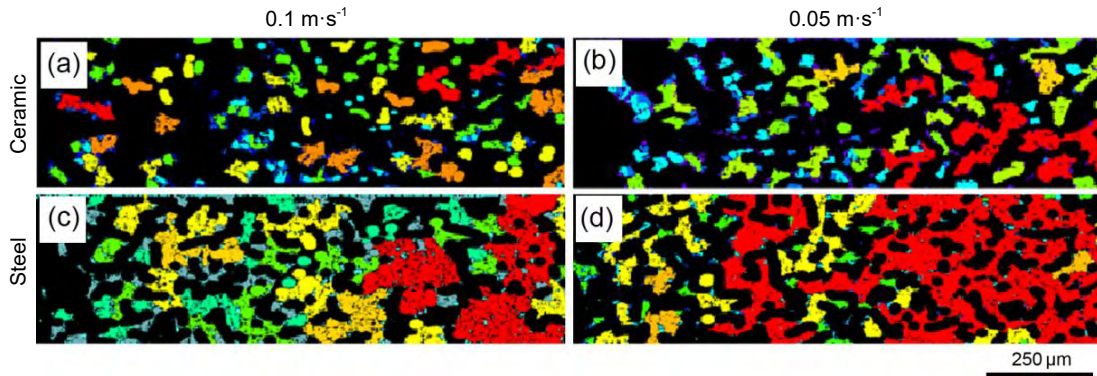


Fig. 5: Distribution of ESCs (extracted from Avizo software) from the surface to the center: (a) T3; (b) T4; (c) T23; (d) T24

### 3.2 Pore analysis

Figure 6 presents the average pore size and central porosity of samples across different processes. Using a ceramic shot sleeve and a higher slow shot speed effectively reduces both average pore size and porosity. By increasing the slow shot speed, the average size of pores inside the casting is significantly reduced. When the slow shot speed increases from  $0.05 \text{ m}\cdot\text{s}^{-1}$  to  $0.1 \text{ m}\cdot\text{s}^{-1}$ , the average size of pores inside the casting prepared by the steel shot sleeve decreases from  $35.3 \mu\text{m}$  to  $17.6 \mu\text{m}$  (a reduction of 49.9%), and the volume fraction of pores also decreases from  $1.18 \times 10^{-4}$  to  $1.06 \times 10^{-4}$  (a reduction of 10.2%). Similar results are also achieved in the ceramic shot sleeve. The internal volume fraction of pores in the samples prepared by the steel shot sleeve is nearly ten times higher than that of the ceramic shot sleeve castings under the same HPDC process conditions. Therefore, it can be concluded that the sensitivity of porosity to the sleeve material is considerably greater than that to the slow shot speed.

### 3.3 Mechanical properties

According to the data obtained from the tensile test, the histograms of the average yield strength, tensile strength, and elongation of the samples in the ceramic shot sleeve and the steel shot sleeve were drawn. The results are shown in Fig. 7.

Samples produced using a ceramic shot sleeve exhibit significantly enhanced performance compared to those made with a steel shot sleeve. When the slow shot speed is set at  $0.1 \text{ m}\cdot\text{s}^{-1}$ , remarkable improvements are observed in the

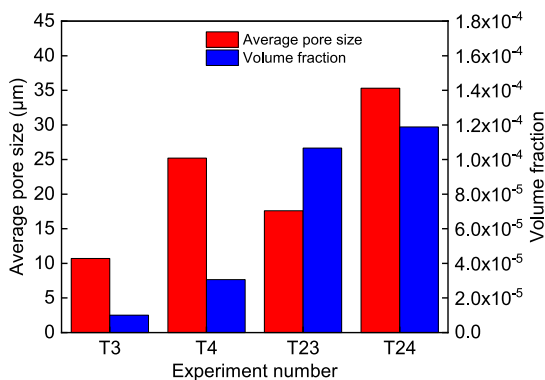


Fig. 6: Volume fraction and average size of pores under different processes

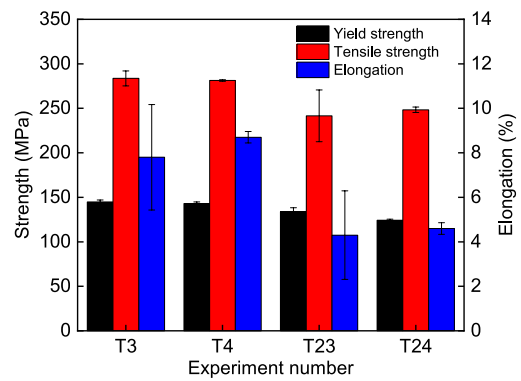


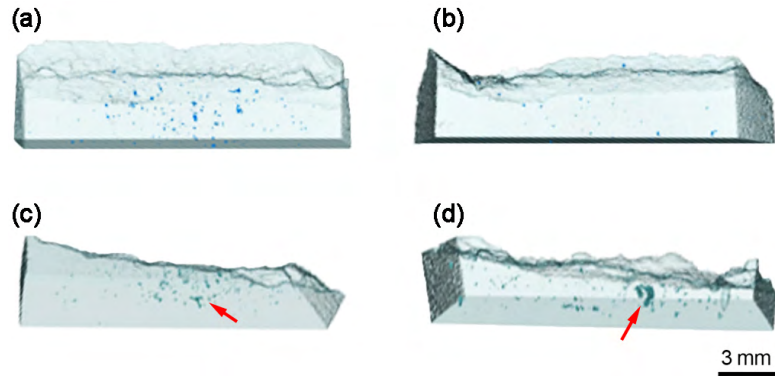
Fig. 7: Mechanical properties of samples with different processes

mechanical properties of the THAS-3 alloy. Specifically, the yield strength increases by 8.3%, the tensile strength surges by 17.4%, and the elongation exhibits an 81.4% growth. However, the slow shot speed has no significant effect on mechanical properties of THAS-3 alloy. The refined ESCs (Fig. 4) and the reduced porosity (Fig. 6) prepared by ceramic shot sleeve contribute to higher strength and elongation.

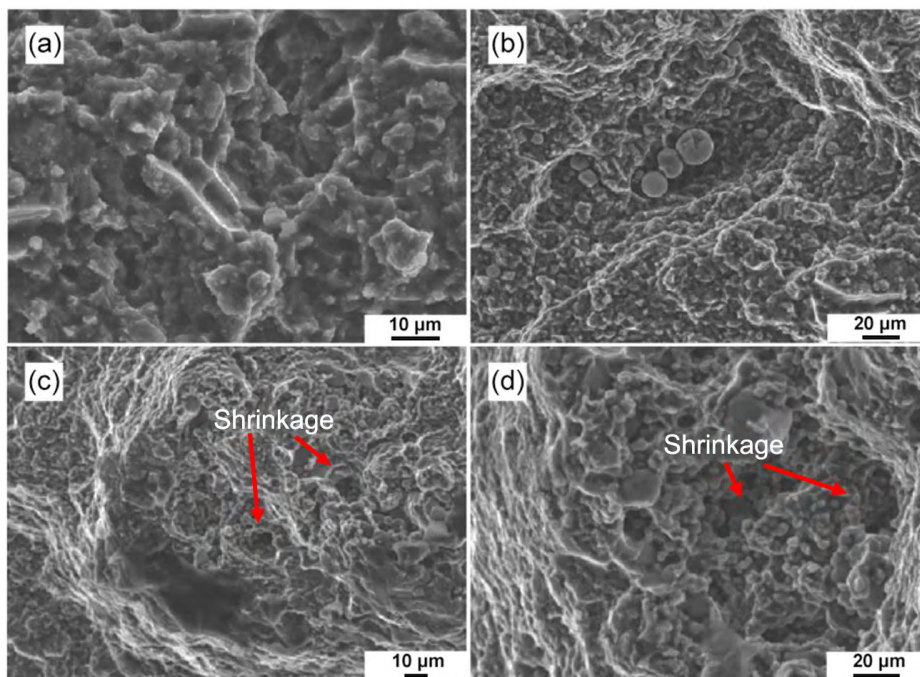
### 3.4 Fracture behavior analysis

Figure 8 shows 3D fracture morphology of die casting THAS-3 alloys under varied HPDC processes. It is not difficult to see that fewer disperse pores exhibit in the samples produced by ceramic shot sleeve [Figs. 8(a) and (b)]. In contrast, the samples prepared by the steel shot sleeve exhibit higher porosity and they are densely distributed around the fracture surface [Figs. 8(c) and (d)]. Particularly, large-sized and interconnected pores are found near the fracture surface under the slow shot speed of  $0.05 \text{ m}\cdot\text{s}^{-1}$ , as shown in Fig. 8(d), which has a great negative impact on the mechanical properties. Combined with the difference in tensile properties of two types of shot sleeve materials given in Table 3, it can be concluded that the use of ceramic shot sleeve for HPDC can effectively reduce the internal pores and improve the mechanical properties of the THAS-3 alloy.

Figure 9 shows the fracture morphology of die casting THAS-3 alloy. It can be observed that the fracture morphology of the samples prepared by ceramic shot sleeve [Figs. 9(a) and (b)] is relatively flat. However, in the samples prepared by



**Fig. 8: 3D fracture morphology of die casting THAS-3 alloy under different HPDC processes: (a)  $0.1 \text{ m}\cdot\text{s}^{-1}$ , ceramic shot sleeve; (b)  $0.05 \text{ m}\cdot\text{s}^{-1}$ , ceramic shot sleeve; (c)  $0.1 \text{ m}\cdot\text{s}^{-1}$ , steel shot sleeve; (d)  $0.05 \text{ m}\cdot\text{s}^{-1}$ , steel shot sleeve**



**Fig. 9: Fracture morphology of die casting THAS-3 alloy under different HPDC processes: (a) T3; (b) T4; (c) T23; (d) T24**

the steel shot sleeve, there are obvious shrinkage and coarse ESCs at the fracture surface, which deteriorates the fracture performance [Figs. 9(c) and (d)]. During the tensile process, shrinkages near the boundaries of larger-sized ESCs are prone to crack initiation due to their reduced ability to withstand significant plastic deformation. The observation results indicate that the samples produced using a steel shot sleeve exhibit a predominant intergranular fracture mode, particularly in the central area of the casting.

## 4 Conclusions

In this study, the microstructure of ESCs, porosity, and mechanical properties of AlSi9MnVTiMgZn alloy prepared by ceramic shot sleeve and steel shot sleeve were studied. Conclusions are drawn as follow:

(1) Compared to castings produced with a steel shot sleeve, those using a ceramic shot sleeve exhibit smaller average ESCs

sizes, particularly at higher slow shot speeds. At  $0.1 \text{ m}\cdot\text{s}^{-1}$ , the ceramic shot sleeve reduces the average ESCs area fraction and size by 52.3% and 6.9%, respectively, versus the steel counterpart.

(2) When the slow shot speed rises from  $0.05 \text{ m}\cdot\text{s}^{-1}$  to  $0.1 \text{ m}\cdot\text{s}^{-1}$ , the pore volume fraction of steel-shot-sleeve samples falls by 10.2%, while that of ceramic-shot-sleeve samples drops by 67.1%. At  $0.1 \text{ m}\cdot\text{s}^{-1}$ , ceramic-shot-sleeve castings have a lower pore volume fraction and smaller pores than steel-shot-sleeve ones.

(3) At a slow shot speed of  $0.1 \text{ m}\cdot\text{s}^{-1}$ , castings produced with a ceramic shot sleeve exhibit 8.3% higher yield strength, 17.4% higher tensile strength, and 81.4% greater elongation than those from a steel shot sleeve. Fracture analysis shows steel-shot-sleeve castings have large ESCs and shrinkage porosity, with obvious intergranular fracture morphology while ceramic-shot-sleeve samples feature a flatter fracture surface.

## Acknowledgments

The authors would like to thank the National Key Research and Development Program of China (Grant No. 2022YFB3404201), the National Natural Science Foundation of China (Grant Nos. 52175335, 52405342), the Natural Science Foundation Joint Foundation of Liaoning province (Grant No. 2023-BSBA-108), and the Fundamental Research Funds for the Central Universities (Grant No. N2402005). The authors also appreciate the help provided by China FAW Foundry Co., Ltd.

## Conflict of interest

Prof. Shou-mei Xiong is an EBM of CHINA FOUNDRY. He was not involved in the peer-review or handling of the manuscript. The authors have no other competing interests to disclose.

## References

- [1] Zhang J H, Niu X D, Qiu X, et al. Effect of yttrium-rich misch metal on the microstructures, mechanical properties and corrosion behavior of die cast AZ91 alloy. *J. Alloys Compd.*, 2009, 471(1): 322–330.
- [2] Hu C Y, Zhu H Y, Wang Y H, et al. Microstructure features and mechanical properties of non-heat treated HPDC Al9Si0.6Mn-TiB<sub>2</sub> alloys. *J. Mater. Res. Technol.*, 2023, 27: 2117–2131.
- [3] Kawajiri K, Kobayashi M, Sakamoto K. Lightweight materials equal lightweight greenhouse gas emission: A historical analysis of greenhouse gases of vehicle material substitution. *J. Cleaner Prod.*, 2020, 253: 119805.
- [4] Senuma T. Physical metallurgy of modern high strength steel sheets. *ISI International*, 2001, 41(6): 520–532.
- [5] Zhang Y, Lai X, Zhu P, et al. Lightweight design of automobile component using high strength steel based on dent resistance. *Mater. Des.*, 2006, 27(1): 64–68.
- [6] Bellamkonda P N, Dwivedy M, Ch K N. Microstructural analysis and preliminary wear assessment of wire arc additive manufactured AA5083 aluminum alloy for lightweight structures. *Int. J. Lightweight Mater. Manuf.*, 2025, 8(1): 1–13.
- [7] Zhang W, Xu J. Advanced lightweight materials for automobiles: A review. *Mater. Des.*, 2022, 221: 110994.
- [8] Harish R S, Sreenivasa Reddy M, Kumaraswamy J. Mechanical behaviour of Al7075 alloy Al<sub>2</sub>O<sub>3</sub>/E-Glass hybrid composites for automobile applications. *Materials Today: Proceedings*, 2023, 72: 2186–2192.
- [9] Luo A A, Sachdev A K, Apelian D. Alloy development and process innovations for light metals casting. *J. Mater. Process. Technol.*, 2022, 306: 117606.
- [10] Dargusch M S, Dour G, Schauer N, et al. The influence of pressure during solidification of high pressure die cast aluminium telecommunications components. *J. Mater. Process. Technol.*, 2006, 180(1): 37–43.
- [11] Zhao H D, Wang F, Li Y Y, et al. Experimental and numerical analysis of gas entrapment defects in plate ADC12 die castings. *J. Mater. Process. Technol.*, 2009, 209(9): 4537–4542.
- [12] Lattanzi L, Fabrizi A, Fortini A, et al. Effects of microstructure and casting defects on the fatigue behavior of the high-pressure die-cast AlSi<sub>9</sub>Cu<sub>3</sub>(Fe) alloy. *Procedia Structural Integrity*, 2017, 7: 505–512.
- [13] Li X, Xiong S M, Guo Z. Correlation between porosity and fracture mechanism in high pressure die casting of AM60B alloy. *J Mater Sci Technol.*, 2016, 32(1): 54–61.
- [14] Liu R X, Zheng J, Godlewski L, et al. Influence of pore characteristics and eutectic particles on the tensile properties of Al-Si-Mn-Mg high pressure die casting alloy. *Mater. Sci. Eng. A*, 2020, 783: 139280.
- [15] Yang Y T, Huang S Y, Zheng J, et al. Effect of porosity and α-Al(Fe/Mn)Si phase on ductility of high-pressure die-casting Al-7Si-0.2Mg alloy. *Trans. Nonferrous Met. Soc. China*, 2024, 34(2): 378–391.
- [16] Jiao X Y, Zhang Y F, Wang J, et al. Characterization of externally solidified crystals in a high-pressure die-cast AlSi10MnMg alloy and their effect on porosities and mechanical properties. *J. Mater. Process. Technol.*, 2021, 298: 117299.
- [17] Zheng H T, Jiang Y H, Liu F, et al. Synergistic effect of externally solidified crystals and Fe-rich intermetallic on the fracture behavior of HPDC alloy. *J. Mater. Res. Technol.*, 2023, 27: 2822–2832.
- [18] Zhang Y, Lordan E, Dou K, et al. Influence of porosity characteristics on the variability in mechanical properties of high pressure die casting (HPDC) AlSi7MgMn alloys. *J. Manuf. Processes.*, 2020, 56: 500–509.
- [19] Zheng H T, Jiang Y H, Liu F, et al. Microstructure heterogeneity optimization of HPDC Al-Si-Mg-Cu alloys by modifying the characteristic of externally solidified crystals. *J. Alloys Compd.*, 2024, 976: 173167.
- [20] Mitrović D, Terčelj M, Kastelic S, et al. Analysis of degradation processes on shot sleeves made from new Si-Mo cast iron in aluminium high pressure die casting – A case study. *Eng. Fail. Anal.*, 2020, 109: 104283.
- [21] Liu Y X, Zhang Y F, Liu W N, et al. Enhanced mechanical properties and thermal conductivity of high-pressure die-cast AlMg6Si2MnZr alloy by controlling the externally solidified crystals. *J. Mater. Process. Technol.*, 2022, 306: 117645.
- [22] Aaronson H I, Kinsman K R, Russell K C. The volume free energy change associated with precipitate nucleation. *Scripta Metallurgica*, 1970, 4(2): 101–106.
- [23] Li J, Nishioka K, Holcomb E R C. Thermodynamic analysis of the driving force for forming a critical nucleus in multicomponent nucleation. *J. Cryst. Growth.*, 1997, 171(1): 259–269.